*Electrochemical and Solid-State Letters*, **7** (9) A259-A263 (2004)
0013-4651/2004/7(9)/A259/5/$7.00 © The Electrochemical Society, Inc.



# A Boundary Condition for Porous Electrodes

**Venkat R. Subramanian,[a,*,z] Deepak Tapriyal,[a] and Ralph E. White[b,**]**

[a]*Department of Chemical Engineering, Tennessee Technological University, Cookeville, Tennessee 38501, USA*
[b]*Department of Chemical Engineering, University of South Carolina, Columbia, South Carolina 29208, USA*

A boundary condition for electrolyte concentration at the porous electrode/separator interface is developed. This boundary condition helps predict the electrolyte concentration profile in the porous electrode without having to solve for the concentration profile in the separator.


Manuscript submitted October 8, 2003; revised manuscript received January 1, 2004. Available electronically July 23, 2004.

Electrochemical models that predict the performance of batteries accurately are usually complex because of the nonlinear coupling of the dependent variables in the governing equations.[1,2] These models have been used by various researchers to optimize the cell design, study the effect of system parameters and thermal behavior. Modeling of electrochemical behavior of secondary batteries (like lithium-ion batteries) involves solving electrolyte concentration and electrolyte potential in the separator; and electrolyte concentration, electrolyte potential, solid-state concentration, and solid-state potential in the porous electrode.[1,2] Even when one-dimensional transport (in $x$) is considered, these models involve two coupled nonlinear partial differential equations (in $x$, $t$) in the separator and three coupled nonlinear partial differential equations (in $x$, $t$) in the porous electrode.[1,2] In addition, solid-state diffusion should be solved in the pseudodimension ($r$, $t$) in the porous electrode. For predicting the thermal behavior, one must add an additional equation for temperature in both the separator and the porous electrode.

Analytical solutions for the mathematical models of Li-ion batteries are available for very few limiting cases.[3,4] Doyle and Newman[3] presented a few limiting cases and analyzed the electrochemical behavior of Li-ion batteries using these simplified models under certain operating conditions. Complexity of the models (and hence the need for numerical solution) arises due to one or more of the following reasons: (*i*) nonlinear coupling between the electrolyte potential and electrolyte concentration (concentrated solution theory); (*ii*) nonlinear Butler-Volmer kinetics, (*iii*) nonlinear dependence of exchange current on the electrolyte or solid-state concentration, (*iv*) nonlinear dependence of open-circuit potential on the solid-state concentration, (*v*) dependence of electrolyte conductivity or electrolyte diffusion coefficient on the electrolyte concentration, (*vi*) dependence of solid-state diffusion coefficient on the solid-state concentration, and (*vii*) dependence of transfer number on the electrolyte concentration. Typically, Li-ion battery models are complicated because of a combination of more than one of the above reasons.

A Li-ion cell sandwich consists of a lithium foil, separator, and a porous electrode.[1,2] To obtain the concentration profiles in the porous electrode, one must solve for the concentration in the profiles in both the separator and the porous electrode. Even when the potential drop in the porous electrode dominates the net voltage of the cell sandwich, one must solve for the equations in both separator and porous electrode. This is true because the boundary condition for the electrolyte concentration at the porous electrode/separator interface is not known. In this article, we arrive at this boundary condition by modeling galvanostatic discharge behavior of a Li-ion cell sandwich under solution-phase diffusion limitations.

* Electrochemical Society Active Member.
** Electrochemical Society Fellow.
z E-mail: vsubramanian@tntech.edu

## Theoretical Development

The geometry modeled is shown in Fig. 1. The cell consists of a lithium-ion foil, a microporous separator, and a porous electrode (*e.g.*, carbon or $LiMn_2O_4$). The following assumptions are made: (*i*) discharge behavior is dominated by solution-phase diffusion limitations,[3] (*ii*) kinetic and diffusion-phase limitations are negligible, and (*iii*) diffusion coefficient and transfer number are independent of the electrolyte concentration.

In the absence of potential gradients and under uniform current distribution, the electrolyte concentration is governed by simplified equations.[3,4] The geometry modeled consists of two regions, a separator ($0 < x < L_s$) and a porous electrode ($L_s < x < L_s + L_c$). The concentration of electrolyte in the separator ($c_1$, mol/m$^3$) is governed by Fick's law of diffusion

$$\frac{\partial c_1}{\partial t} = D\frac{\partial^2 c_1}{\partial x^2} \quad [1]$$

where $D$ is the diffusion coefficient (m$^2$/s) of the electrolyte. A material balance governs the concentration of electrolyte ($c_2$, mol/m$^3$) in the porous electrode

$$\varepsilon\frac{\partial c_2}{\partial t} = D\varepsilon^{1.5}\frac{\partial^2 c_2}{\partial x^2} + aj_n(1 - t^+) \quad [2]$$

where $\varepsilon$ is the porosity of the electrode, $a$ is the specific interfacial area (m$^{-1}$), and $j_n$ is the pore wall flux of lithium ions (mol/m$^2$/s). Note that the Bruggeman expression has been used for obtaining the effective diffusivity in the electrolyte.[5]

Uniform initial conditions are assumed throughout the sandwich

$$c_1 = c_2 = c_0 \text{ at } t = 0 \quad [3]$$

For a galvanostatic discharge, the rate of discharge governs the mass flux at $x = 0$ (Li foil)

$$\frac{\partial c_1}{\partial x} = -\frac{I(1 - t^+)}{nDF} \text{ at } x = 0 \quad [4]$$

where $I$ is the current density (A/m$^2$), $n$ is the number of electrons transferred in the electrochemical reaction ($n = 1$ here), and $F$ is the Faraday constant. The mass flux is zero at the current collector ($x = L_s + L_c$)

$$\frac{\partial c_2}{\partial x} = 0 \text{ at } x = L_s + L_c \quad [5]$$

Concentration and mass flux are continuous at the separator-porous electrode interface ($x = L_s$)

$$c_1 = c_2 \text{ at } x = L_s \quad [6]$$

and

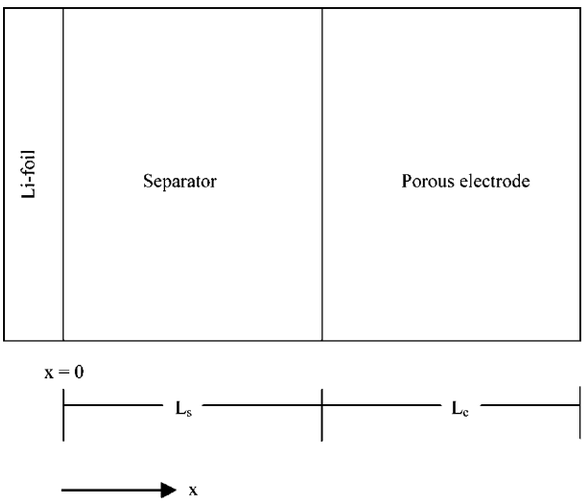


**Figure 1.** Lithium-ion cell sandwich, consisting of lithium-foil, separator, and porous electrode.

$$\frac{\partial c_1}{\partial x} = \varepsilon^{3/2}\frac{\partial c_2}{\partial x} \text{ at } x = L_s \quad [7]$$

Equations 1-7 govern the concentration distributions in the cell sandwich (separator and porous electrode).

When the open-circuit potential depends strongly on the state of charge of the system or when kinetic resistances dominate ohmic resistances,[3,4] it is possible to assume that $j_n$ is given by its average value everywhere in the porous electrode

$$j_n = -\frac{I}{aFL_c} \quad [8]$$

When Eq. 8 is substituted in Eq. 2 we get

$$\varepsilon\frac{\partial c_2}{\partial t} = D\varepsilon^{1.5}\frac{\partial^2 c_2}{\partial x^2} - \frac{I(1 - t^+)}{nFL_c} \quad [9]$$

The following dimensionless variables are introduced

$$C_1 = \frac{c_1}{c_0}$$

$$C_2 = \frac{c_2}{c_0}$$

$$X = \frac{x}{L_s}$$

$$\tau = \frac{Dt}{L_s^2}$$

$$r = \frac{L_c}{L_s} \quad [10]$$

The governing equations and boundary conditions are converted to dimensionless form using Eq. 10 as follows

$$\frac{\partial C_1}{\partial \tau} = \frac{\partial^2 C_1}{\partial X^2} \text{ for } 0 < X < 1 \quad [11]$$

$$\frac{\partial C_2}{\partial \tau} = \sqrt{\varepsilon}\frac{\partial^2 C_2}{\partial X^2} + J \quad \text{for } 1 < X < r \quad [12]$$

where $J$ is the dimensionless current density given by

**Table I. Values of parameters used in the simulation.**

| Parameters | Value | Parameters | Value |
|---|---|---|---|
| $D$ | $2.6 \times 10^{-10}$ m$^2$/s | $\varepsilon$ | 0.35 |
| $I_{app}$ | 60 A/m$^2$ | $L_s$ | 25 μm |
| $F$ | 96,487 | $L_c$ | 125 μm |
| $t^+$ | 0.20 | $c_0$ | 1000 mol/m$^3$ |

$$J = -\frac{I(1 - t^+)L_s^2}{FDL_c c_0 \varepsilon} \quad [13]$$

The dimensionless initial condition is

$$C_1 = C_2 = 1 \text{ at } \tau = 0 \quad [14]$$

The dimensionless boundary conditions are

$$\frac{\partial C_1}{\partial X} = J\varepsilon r \text{ at } X = 0 \quad [15]$$

$$\frac{\partial C_2}{\partial X} = 0 \text{ at } X = 1 + r \quad [16]$$

$$C_1 = C_2 \text{ at } X = 1 \quad [17]$$

$$\frac{\partial C_1}{\partial X} = \varepsilon^{3/2}\frac{\partial C_2}{\partial X} \text{ at } X = 1 \quad [18]$$

Equations 11 and 12 can be solved analytically using the separation of variables method.[3,6] Typical values of parameters are used for the simulation and are listed in Table I.[7]

## Approximate Model

We can predict the concentration profile in the porous electrode by solving for the concentration equation in the porous electrode alone. To do this, we need the boundary condition at the porous electrode/separator interface. We arrive at this boundary condition in this section.

The dimensionless concentration in the separator is assumed to be a parabolic polynomial in $X$[8]

$$C_1 = a + bX + eX^2 \quad [19]$$

where $a$, $b$, and $e$ are functions of time and are obtained from the governing equations and boundary conditions. The governing equation is satisfied in an average sense. That is Eq. 19 is substituted into the equation for $C_1$ (Eq. 11) and integrated from 0 to 1 to obtain

$$\frac{d(a)}{dt} + \frac{d(b)}{2dt} + \frac{d(e)}{3dt} = 2e \quad [20]$$

The average concentration in the separator ($\overline{C_1}$) is obtained by integrating Eq. 19 from 0 to 1

$$\overline{C_1} = a + \frac{b}{2} + \frac{e}{3} \quad [21]$$

Using the boundary condition at $X = 0$ (Eq. 15) and Eq. 19 we get

$$b = rJ\varepsilon \quad [22]$$

Substituting Eq. 19 in 17 we get

$$a + b + e = C_2 \text{ at } X = 1 \quad [23]$$

Using Eq. 20, 22, and 23 we can calculate $a$, $b$, and $e$. Equation 18 is simplified as

$$\varepsilon^{1.5}\frac{\partial C_2}{\partial X} = -\frac{rJ\varepsilon}{2} + 3C_2 - 3\overline{C_1} \quad [24]$$

where $\overline{C_1}$ is obtained by substituting *a*, *b*, and *e* in Eq. 21

$$\frac{d\overline{C_1}}{d\tau} = -\frac{3rJ\varepsilon}{2} + 3C_2 - 3\overline{C_1} \quad [25]$$

Because the boundary condition at the interface is known, the concentration profile in the porous electrode is obtained by solving the following governing equation

$$\frac{\partial C_2}{\partial \tau} = \sqrt{\varepsilon}\frac{\partial^2 C_2}{\partial Z^2} + J \text{ for } Z = 0 \text{ to } r \quad [26]$$

where $Z = X - 1$ and the boundary conditions are

$$\varepsilon^{1.5}\frac{\partial C_2}{\partial Z} = -\frac{rJ\varepsilon}{2} + 3C_2 - 3\overline{C_1} \text{ at } Z = 0 \quad [27]$$

$$\frac{\partial C_2}{\partial Z} = 0 \text{ at } Z = r \quad [28]$$

In addition, $\overline{C_1}$ is governed by Eq. 25. The initial conditions are

$$\overline{C_1} = C_2 = 1 \text{ at } \tau = 0 \quad [29]$$

Next, to simplify the governing equations further we introduce $C_2 = 1 + Ju_2$ and $\overline{C_1} = 1 + J\overline{u_1}$ to obtain the following equations

$$\frac{\partial u_2}{\partial \tau} = \sqrt{\varepsilon}\frac{\partial^2 u_2}{\partial Z^2} + 1 \quad [30]$$

$$\varepsilon^{1.5}\frac{\partial u_2}{\partial Z} = -\frac{r\varepsilon}{2} + 3u_2 - 3\overline{u_1} \text{ at } Z = 0 \quad [31]$$

$$\frac{\partial u_2}{\partial Z} = 0 \text{ at } Z = 1 \quad [32]$$

$$\frac{d\overline{u_1}}{d\tau} = -\frac{3r\varepsilon}{2} + 3u_2 - 3\overline{u_1} \quad [33]$$

$$\overline{u_1} = u_2 = 0 \text{ at } \tau = 0 \quad [34]$$

Equation 30 is solved in the Laplace domain with the boundary condition at $Z = 0$ (Eq. 31)

$$u_2(s) = q\cosh\left(\frac{\sqrt{s}(r - Z)}{\varepsilon^{(1/4)}}\right) + \frac{1}{s^2} \quad [35]$$

where

$$q = \frac{s\varepsilon r - 6(1 + \varepsilon r)}{2s^{3/2}\left[\varepsilon^{5/4}\sinh\left(\frac{s^{1/2}r}{\varepsilon^{1/4}}\right)(s + 3) + 3\sqrt{s}\cosh\left(\frac{s^{1/2}r}{\varepsilon^{1/4}}\right)\right]} \quad [36]$$

Equation 35 is inverted to the time domain by using the Heaviside expansion theorem[9] as follows

$$u_2 = w_2 + \sum_{n=1}^{\infty} A_n\cos\left(\frac{\lambda_n(r - Z)}{\varepsilon^{1/4}}\right)\exp(-\lambda_n^2\tau) \quad [37]$$

where $w_2$ is the steady-state profile given by

$$w_2 = \frac{\varepsilon r^3 + 3r^2 + 3r\varepsilon^{3/2} - 3(1 + \varepsilon r)(r - Z)^2}{6(1 + \varepsilon r)\sqrt{\varepsilon}} \quad [38]$$

**Table II. Values of eigenvalues and coefficients for $r$=5, $\varepsilon$=0.35.**

| $\lambda_n$ (Eq. 39) | $n$ | $A_n$ (Eq. 40) |
|---|---|---|
| 0.3414 | 0 | −13.8967 |
| 0.7672 | 1 | 1.7773 |
| 1.2225 | 2 | −0.5095 |
| 1.6926 | 3 | 0.22124 |
| 2.164 | 4 | −0.1219 |
| 2.6375 | 5 | 0.07799 |

and the eigenvalues are calculated using the transcendental equation

$$\varepsilon^{5/4}\sin\left(\frac{\lambda_n r}{\varepsilon^{1/4}}\right)(\lambda_n^2 - 3) - 3\cos\left(\frac{\lambda_n r}{\varepsilon^{1/4}}\right)\lambda_n = 0 \quad \text{for } n = 1,2,... \propto \quad [39]$$

The coefficient $A_n$ in Eq. 37 is obtained by using the method of residues as[6,9]

$$A_n = \frac{P}{\left(\frac{dQ}{ds}\right)_{s=-\lambda_n^2}} \quad \text{for } n = 1,2,... \propto \quad [40]$$

where $P$ is the numerator and $Q$ is the denominator of $q$ defined in Eq. 36. Numerical values of $A_n$ and $\lambda_n$ for $\varepsilon = 0.35$, $r = 5$ are given in Table II. Note that both eigenvalues and coefficients are independent of $J$, the dimensionless current density. Substituting the value of $u_2$ in $C_2 = 1 + Ju_2$ we get

$$C_2 = 1 + J\left(w_2 + \sum_{n=1}^{\infty} A_n\cos\left(\frac{\lambda_n(r - Z)}{\varepsilon^{1/4}}\right)\exp(-\lambda_n^2\tau)\right) \quad [41]$$

The steady-state profile in the porous electrode may be obtained by neglecting the transient term in Eq. 41 as

$$C_{2,\tau=\infty} = 1 + Jw_2 = 1 + J\frac{\varepsilon r^3 + 3r^2 + 3r\varepsilon^{3/2} - 3(1 + \varepsilon r)(1 + r - X)^2}{6(1 + \varepsilon r)\sqrt{\varepsilon}} \quad [42]$$

## Average Concentration and Steady-State Concentration Profiles

Unlike common transient diffusion models,[10] the exact model (Eq. 11-18) cannot be solved to obtain the steady-state profile by equating the transient terms to zero. This is true because the solution of steady-state versions of Eq. 11 and 12 involves four constants of integration of which only three can be found using the boundary conditions defined in Eq. 15-18.[3,6] To find the fourth constant of integration, Eq. 11 and 12 are integrated as

$$\int_0^1 \frac{\partial C_1}{\partial \tau}dX = \left(\frac{\partial C_1}{\partial X_{X=1}} - \frac{\partial C_1}{\partial X_{X=0}}\right) \quad [43]$$

and

$$\int_1^{1+r} \frac{\partial C_2}{\partial \tau}dX = \sqrt{\varepsilon}\left(\frac{\partial C_2}{\partial X_{X=1+r}} - \frac{\partial C_2}{\partial X_{X=1}}\right) + Jr \quad [44]$$

If we denote the average concentration in the separator and the electrode as $\overline{C_1}$ and $\overline{C_2}$, respectively, Eq. 43 and 44 can be combined to obtain

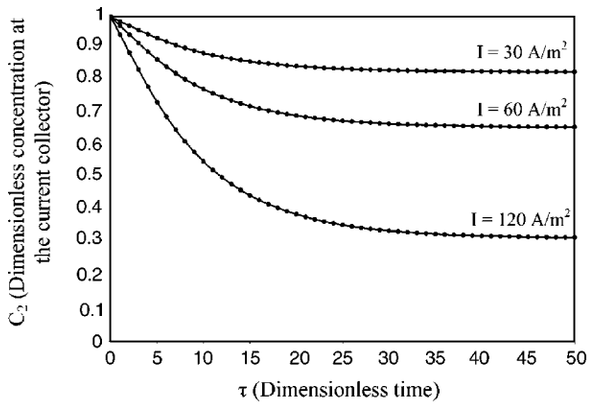


**Figure 2.** Dimensionless concentration at the current collector is plotted against dimensionless time for different rates of discharge. The solid lines represent the exact model (Eq. 11-18) and the dotted lines represent the approximate solution developed (Eq. 41). 1C rate corresponds to 60 A/m$^2$.

$$\frac{d\overline{C_1}}{d\tau} + \varepsilon r \frac{d\overline{C_2}}{d\tau} = 0 \qquad [45]$$

Equation 45 can be integrated using the initial condition (Eq. 14) to get

$$\overline{C_1} + \varepsilon r \overline{C_2} = 1 + \varepsilon r \qquad [46]$$

Steady-state versions of Eq. 11 and 12 can be solved with Eq. 15, 17, 18, and 46 to obtain the steady-state concentration profiles as

$$C_{1,\tau=\infty} = 1 - J\varepsilon r\left(1 - X - \frac{1}{2(1+\varepsilon r)} + \frac{r^2}{3\sqrt{\varepsilon}(1+\varepsilon r)}\right) \qquad [47]$$

and

$$C_{2,\tau=\infty} = 1 + J\frac{\varepsilon r^3 + 3r^2 + 3r\varepsilon^{3/2} - 3(1+\varepsilon r)(1+r-X)^2}{6\sqrt{\varepsilon}(1+\varepsilon r)} \qquad [48]$$

We observe that the steady-state concentration profile in the porous electrode obtained using the exact model (Eq. 48) matches exactly with the steady-state profile obtained with the approximate model (Eq. 42).

## Results and Discussion

The profiles obtained from the simplified model are compared with the exact model (Eq. 11-18) in Fig. 2 and 3. The dimensionless concentration at the current collector is plotted as a function of dimensionless time for 30, 60, and 120 A/m$^2$ rates using both the approximate model developed and the exact model (Eq. 11-18) in Fig. 2. We observe that the approximate model predicts the concentration profiles accurately. We observe that the dimensionless concentration decreases with time for a given rate of discharge, and approaches a steady state. In addition, we observe that the dimensionless concentration decreases faster for higher rates of discharge.

The dimensionless concentration at the porous electrode/separator interface is plotted as a function of dimensionless time for 30, 60, and 120 A/m$^2$ in Fig. 3. We observe that the approximate model predicts the concentration profiles accurately. We observe that the dimensionless concentration at the electrode/separator interface increases with time for a given rate of discharge, and approaches a steady state. In addition, we observe that the dimensionless concentration increases faster for higher rates of discharge.

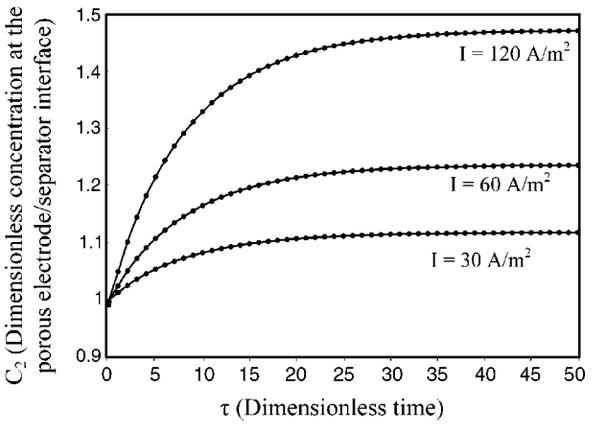


**Figure 3.** Dimensionless concentration at the electrode-separator interface is plotted against dimensionless time for different rates of discharge. The solid lines represent the exact model (Eq. 11-18) and the dotted lines represent the approximate solution developed (Eq. 41). 1C rate corresponds to 60 A/m$^2$.

The dimensionless concentration at the porous electrode/separator interface is plotted as a function of dimensionless time for different values of $r$ (ratio of electrode length to the separator length) in Fig. 4. We observe that for higher values of $r$, the dimensionless concentration depletes faster. From Fig. 2, 3, and 4 we conclude that the approximation is good and may be used with no loss of accuracy.

The methodology and boundary condition developed for concentration at the separator/porous electrode interface in this article can be extended to more realistic models. This is true because even for complicated models the governing equation for concentration in the separator is very similar to Eq. 1.[1,2] Hence, the boundary condition developed for electrolyte concentration at the porous electrode/separator interface (Eq. 31) may be used for complicated models also. In addition, the boundary conditions for the electrolyte potential and solid-phase potential at the porous electrode/separator interface are known accurately because the entire current is carried by the electrolyte phase at the interface.[1,2] In our next paper, we plan to predict the discharge behavior of the cell sandwich by solving for governing equations in the porous electrode alone without solving for the profiles in the separator. The boundary condition developed in this paper should also find use in theoretical analysis of porous

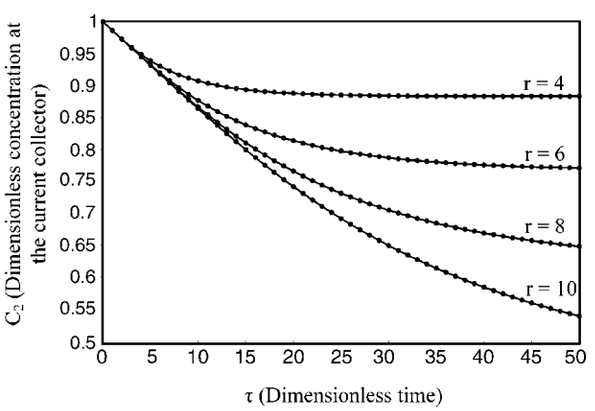


**Figure 4.** Dimensionless concentration at the current collector plotted against dimensionless time for different values of $r$ (ratio of electrode length to separator length) at the 1C rate of discharge (60 A/m$^2$). The solid lines represent the exact model (Eq. 11-18) and the dotted lines represent the approximate solution developed (Eq. 42).

electrodes and impedance simulation of porous electrodes. We plan to publish this later.

## Acknowledgments

The authors are grateful for the financial support of the project by National Reconnaissance Organization (NRO) under contract NRO 000-03-C-0122. The authors also acknowledge the Center for Electric Power, Tennessee Tech University, for providing a research assistantship to D.T.

*The University of South Carolina assisted in meeting the publication costs of this article.*

## List of Symbols

| | |
|---|---|
| $a$ | interfacial area, $m^{-1}$ |
| $c$ | concentration of the electrolyte, $mol/m^3$ |
| $t$ | time, s |
| $x$ | distance, m |
| $D$ | diffusion coefficient of the electrolyte, $m^2/s$ |
| $j_n$ | pore wall flux of Li ions, $mol/m^2/s$ |
| $t^+$ | transfer number |
| $I$ | current density, $A/m^2$ |
| $L_c$, $L_s$ | length of the electrode, m, length of the separator, m |
| $F$ | Faraday's law constant, 96,487 C/g equiv |
| $C$,$u$ | dimensionless concentration, $c/c_0$ |
| $X$,$Z$ | dimensionless distance, $X = x/L$, $Z = X - 1$ |
| $J$ | dimensionless current density (see Eq. 13) |
| $r$ | ratio of thickness of the electrode to the thickness of the separator, $L_c/L_s$ |
| $n$ | number of electrons transferred ($n = 1$ for the simulation) |
| $\overline{C_1}$, $\overline{u_1}$ | dimensionless average concentration (see Eq. 21) |

Greek

| | |
|---|---|
| $\varepsilon$ | porosity of the electrode |
| $\lambda_n$ | eigenvalues |
| $\tau$ | dimensionless time, $\tau = Dt/L_c^2$ |

ubscripts

| | |
|---|---|
| 0 | initial condition |
| 1 | separator |
| 2 | porous electrodes |

## References

1. M. Doyle, T. F. Fuller, and J. Newman, *J. Electrochem. Soc.*, **140**, 1526 (1993).
2. G. G. Botte, V. R. Subramanian, and R. E. White, *Electrochim. Acta*, **45**, 2595 (2000).
3. M. Doyle and J. Newman, *J. Appl. Electrochem.*, **27**, 846 (1997).
4. J. S. Newman, *Electrochemical Systems*, pp. 454-495, Prentice Hall, Englewood Cliffs, NJ (1991).
5. D. A. G. Bruggeman, *Appl. Phys.*, **24**, 636 (1935).
6. V. R. Subramanian and R. E. White, *J. Power Sources*, **96**, 385 (2001).
7. G. G. Botte and R. E. White, *J. Electrochem. Soc.*, **148**, A54 (2001).
8. V. R. Subramanian, J. A. Ritter, and R. E. White, *J. Electrochem. Soc.*, **148**, E444 (2001).
9. A. Varma and M. Morbidelli, *Mathematical Methods in Chemical Engineering*, pp. 568-574, Oxford University Press, New York (1997).
10. J. Crank, *Mathematics of Diffusion*, pp. 44-47, Oxford University Press, New York (1975).